GEOLOGY | THE GEOLOGICAL SOCIETY OF AMERICA®

https://doi.org/10.1130/G46977.1

Manuscript received 14 April 2019
Revised manuscript received 8 November 2019
Manuscript accepted 12 November 2019

Published online 17 December 2019

Atmospheric dust stimulated marine primary productivity during Earth's penultimate icehouse

Mehrdad Sardar Abadi[1], Jeremy D. Owens[2], Xiaolei Liu[1], Theodore R. Them II[2,3], Xingqian Cui[4], Nicholas G. Heavens[5,6] and Gerilyn S. Soreghan[1]

[1]School of Geosciences, University of Oklahoma, Norman, Oklahoma 73019, USA
[2]Department of Earth, Ocean, and Atmospheric Science, Florida State University, and National High Magnetic Field Laboratory, Tallahassee, Florida 32306, USA
[3]Department of Geology and Environmental Geosciences, College of Charleston, Charleston, South Carolina 29424, USA
[4]Department of Earth Atmospheric and Planetary Sciences, Massachusetts Institute of Technology, Cambridge, Massachusetts 02139, USA
[5]Department of Atmospheric and Planetary Sciences, Hampton University, 21 E. Tyler Street, Hampton, Virginia 23668, USA
[6]Space Science Institute, 4750 Walnut Street, Suite 205, Boulder, Colorado 80301, USA

ABSTRACT

The importance of dust as a source of iron (Fe) for primary production in modern oceans is well studied but remains poorly explored for deep time. Vast dust deposits are well recognized from the late Paleozoic and provisionally implicated in primary production through Fe fertilization. Here, we document dust impacts on marine primary productivity in Moscovian (Pennsylvanian, ca. 307 Ma) and Asselian (Permian, ca. 295 Ma) carbonate strata from peri-Gondwanan terranes of Iran. Autotrophic contents of samples, detected by both point-count and lipid-biomarker analyses, track concentrations of highly reactive Fe, consistent with the hypothesis that dust stimulated primary productivity, also promoting carbonate precipitation. Additionally, highly reactive Fe tracks the fine-dust fraction. Dust-borne Fe fertilization increased organic and inorganic carbon cycling in low- and mid-latitude regions of Pangaea, maintaining low pCO_2.

INTRODUCTION

Atmospheric dust carries nutrients such as iron and fixed nitrogen that fertilize marine primary producers, impacting carbon cycling (e.g., Martin, 1990; Boyd et al., 2004; Krishnamurthy et al., 2010). Today, eolian delivery of nutrients to iron-limited marine systems controls phytoplankton populations (Guo et al., 2012; Chien et al., 2016) and can intensify carbonate precipitation through stimulation of microbial activity (Bressac et al., 2014; Guieu et al., 2014; Swart et al., 2014; Zhu and Dittrich, 2016).

Despite the importance of eolian dust in supplying marine nutrients, the biotic consequences of dust in Earth's deep-time record remain poorly known. Dust deposits are well documented from the late Paleozoic (Soreghan et al., 2008, 2015), with the possibility of large dust-fertilization effects, but evidence is preliminary and limited to the paleo-equator (Sur et al., 2015). Establishing a link between atmospheric dust and productivity that extended to mid-latitudes would clarify global biogeochemical responses and carbon cycling during the late Paleozoic ice age (LPIA). These effects also have implications for Earth's climate projections, given the urgent need to achieve negative carbon emissions (e.g., Hauck et al., 2016; IPCC, 2018).

For the first time in the ancient record, we investigated the relationship among concentrations of dust, bioavailable iron, autotroph content, and bacterial biomarkers from shallow-marine carbonate of the Central Persian terrane (present-day Iran) once located in southeastern mid-latitude Pangaea (Fig. 1A) to assess the strength and spatial extent of the iron-fertilization effect in deep time. The findings have potential implications for the influences of atmospheric dust on carbon cycling in Earth's penultimate icehouse and beyond.

BACKGROUND AND METHODS

Pennsylvanian–Permian carbonate strata of the study area were located at ~30°S at the time of deposition, adjacent to the northeastern Arabian margin of Gondwana, in relative proximity (~1000 km) to Gondwanan ice centers (e.g., Arabian shield; Sardar Abadi et al., 2019). The upper Moscovian of the Sanandaj-Sirjan zone and lower Asselian of the Alborz Basin record deposition of warm, shallow-marine carbonate isolated from fluvial-deltaic sediment sources (Sardar Abadi et al., 2019). These strata record multiple glacioeustatic sequences, and high-resolution (20 cm) sampling was conducted through 28 m of the study intervals to capture several sequences. Petrographic and biomarker data indicate a diverse biotic assemblage including speciose cyanobacteria, phylloid algae, other calcareous green and red algae, and heterozoans, as well as abundant abiotic components.

We point-counted (400 points per sample) thin sections from 21 Asselian and 25 Moscovian samples, selected to capture facies variation. Components were categorized into abiotic, autotrophic, heterotrophic, and symbiotic attributes (following Schlager, 2003; Table DR1 in the GSA Data Repository[1]). In this terminology, "abiotic" refers to physically precipitated carbonate (e.g., ooids), "autotrophic" components are primary producers (e.g., calcareous green algae), "heterotrophic" components are consumers (e.g., bryozoans), and "symbiotic" components are two cooperating organisms,

[1]GSA Data Repository item 2020064, Figures DR1–DR5, Tables DR1 and DR2, and supplemental data set with iron speciation, ICP-MS results, and grain-size analysis, is available online at http://www.geosociety.org/datarepository/2020/, or on request from editing@geosociety.org.

CITATION: Sardar Abadi, M., et al., 2020, Atmospheric dust stimulated marine primary productivity during Earth's penultimate icehouse: Geology, v. 48, p. 247–251, https://doi.org/10.1130/G46977.1

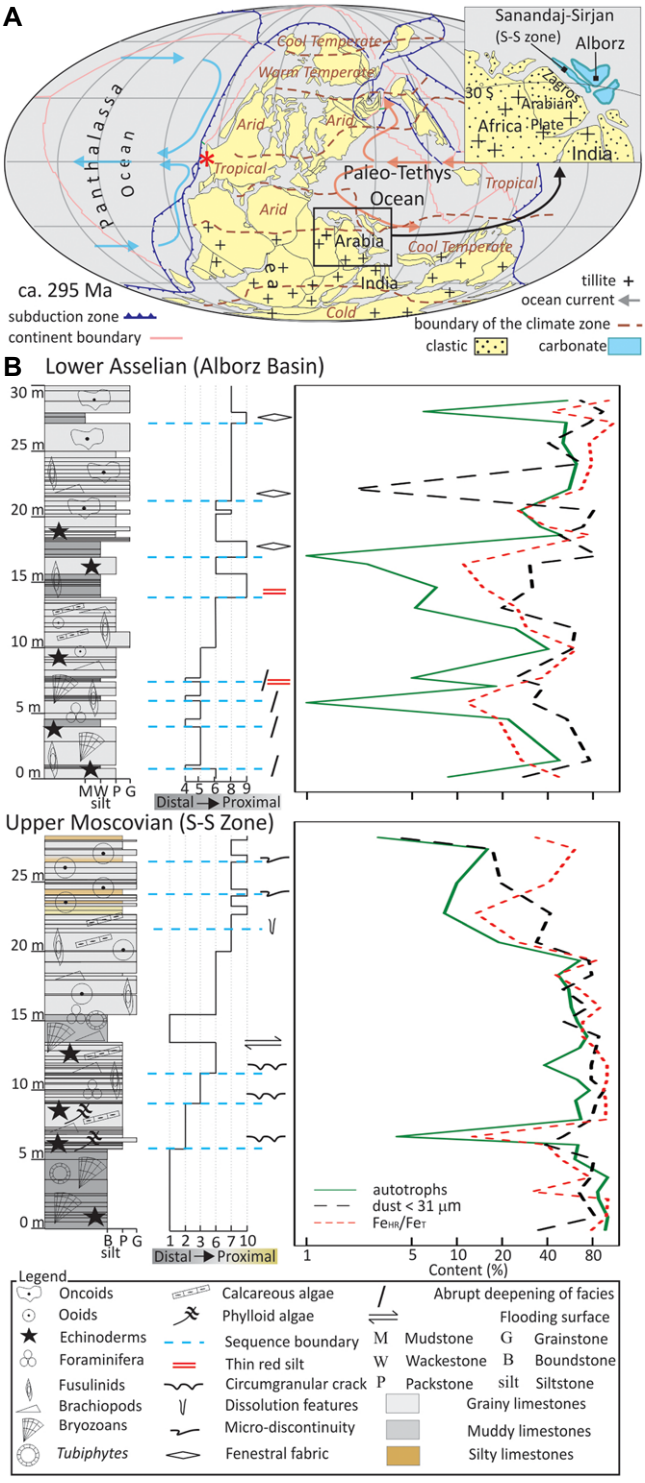

Figure 1. (A) Paleogeographic reconstruction, including climate and oceanic currents during Early Permian time (ca. 295 Ma; modified after Sardar Abadi et al., 2019). Note that present-day Iran (including Alborz, Sanandaj-Sirjan, and central Iran) is traditionally positioned near the Arabian section of the Gondwanan margin. Asterisk (*) indicates paleogeographic location of the Midland Basin sampled by Sur et al. (2015). (B) Facies logs of study sections, Alborz Basin, and Sanandaj-Sirjan zone, including schematic sedimentologic logs with facies and cycle boundaries (horizontal dashed lines). Cycle boundaries were chosen based on the presence of one or more of the following features: evidence for micro-exposure (e.g., circumgranular cracking, alveolar structures, microdiscontinuity), fenestrate fabric, red siltstone, and/or abrupt deepening of facies. Successions record incomplete facies progradation with subtle evidence for subaerial exposure that indicates the influence of high-frequency (inferred glacioeustatic) falls. Plots on the right indicate percent autotroph content, ratio of highly reactive iron to total iron (Fe_{HR}/Fe_T), and percent fine dust (<31 µm) out of total dust. The ratio Fe_{HR}/Fe_T is shown as a percent to graph it on the same x-axis as other values. See Table DR2 (see footnote 1) for facies descriptions and interpretations. Autotroph content significantly increases with Fe_{HR}/Fe_T in the Moscovian (F-test statistic of a linear regression [F] = 15.3, degrees of freedom [df] = (1,23); R^2 = 0.4; p <0.001) and in the Asselian (F = 32, df = (1,19); R^2 = 0.63, p <0.001). Autotroph content significantly increases with fine-grained dust in the Moscovian (F = 15, df = (1,23); R^2 = 0.39; p <0.001). For the Asselian, the relationship between autotroph content and fine-grained dust is less robust, driven primarily by one outlier data point with extremely low fine-grained dust content. Removal of this outlier results in weak positive correlation (F = 3.1, df = (1,18); R^2 = 0.15; p = 0.09). Distal→Proximal means distal facies to proximal facies with respect to the shoreline.

one providing nutrients and one providing carbohydrates (e.g., fusulinids). Additionally, total lipids were extracted from six samples, selected to represent a range of cyanobacterial content based on point-counting; hopanoid biomarkers were targeted for measurements on gas chromatography–mass spectrometry under multiple reaction monitoring (MRM) to evaluate the presence of cyanobacteria, indicated by the ratio of 2-methyl hopane to total hopane, also known as the 2-methyl hopane index (2-MHI) (Summons et al., 1999). All samples (n = 50) were analyzed for bulk-rock geochemistry using inductively coupled plasma–mass spectrometry.

Samples were processed for dust extraction by sequential steps to remove carbonate, organic, pyritic, iron-oxide, and authigenic silica components (Sur et al., 2010); subsequently, the extracted dust was analyzed by laser particle-size analysis (Malvern Mastersizer 3000). A standard sequential extraction (Poulton and Canfield, 2005) was used on (unprocessed) sample splits to assess the amount of highly reactive iron (Fe_{HR}) species (cf. Raiswell et al., 2018). Fe_{HR} is generally determined by summing dithionite iron (Fe_D), acetate iron (Fe_{ac}), oxalate iron (Fe_{OX}) and pyrite iron (Fe_{py}). However, we did not include Fe_{py} in our calculation of Fe_{HR} because samples (n = 5) with petrographic evidence of pyrite documented very low Fe_{py} (0.01–0.03 wt%). The ratio of Fe_{HR} to total iron (Fe_T) is a proxy for initially bioavailable iron; while this approach does not quantify bioavailable iron, this is the best available proxy for quantifying potential ancient iron bioavailability (Sur et al., 2015). Additionally, iron extraction quantifies the various fractions of Fe corresponding to different iron species that are highly reactive. Importantly, Fe_T does not vary appreciably through the analyzed samples, thus the ratio of Fe_{HR} to Fe_T reflects changes in Fe_{HR} in the sample.

We used linear and polynomial regressions to examine relationships between Fe_{HR}/Fe_T and proportions of autotrophic, heterotrophic, symbiotic, and abiotic components. We performed a redundancy analysis (RDA) to examine relationships among Fe_{HR}, dust grain size, and biotic and abiotic components. RDA is an ordination technique that allows hypothesis testing for multiple driver and predictor variables (Legendre and Legendre, 1998). RDA was conducted using the *vegan* package (Oksanen et al., 2018) in the R program version 3.5.3 (R Core Team, 2019). To limit collinearity in our models, we tested for variance inflation factors (VIFs) and included only predictor variables with VIFs <4 (Groß, 2003). Driver variables demonstrated no variance inflation (all VIFs <4).

RESULTS

High-frequency sequences of the study sections generally comprise intervals with high heterotrophic content that, in the Asselian, yield upward to autotroph-dominant, and in the Moscovian, yield to abiotic-dominant facies, with minor evidence for lowstand (incipient exposure) at sequence tops.

Biomarker results of the six samples display a range of 5.5%–12.5% (average 8.0%) for 2-MHI, which indicates the relative proportion of organic matter contributed by cyanobacteria (Summons et al., 1999). These results imply a high influence of cyanobacterial activity for all of our samples.

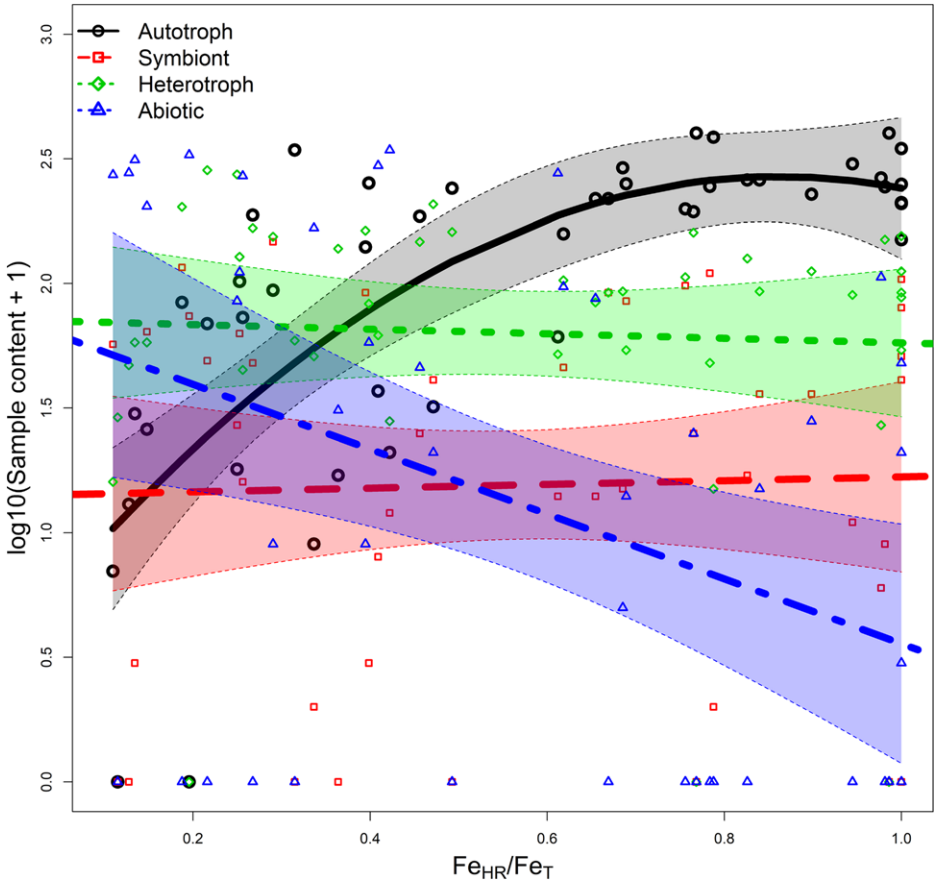

Figure 2. Relationship between proportion of highly reactive Fe over total Fe (Fe_{HR}/Fe_T) and log + 1–transformed count of the number of points containing autotrophs, symbionts, heterotrophs, and abiotic content in peri-Gondwanan terranes of Iran. Colored bands represent 95% confidence intervals. Fe_{HR}/Fe_T correlates significantly with increased sample autotrophic content (R^2 = 0.51; *F*-test statistic of a linear regression [*F*] = 46.7, degrees of freedom [df] = (1,44); *P* <0.001) and decreased abiotic content (R^2 = 0.20; *F* = 10.7, df = (1,44); *P* = 0.002), and had no significant effect on symbiont (R^2 = 0.002; *F* = 0.08, df = (1,44); *P* = 0.78) or heterotrophic content (R^2 = 0.003; *F* = 0.1, df = (1,44); *P* = 0.71). The relationship between community composition and Fe_{HR}/Fe_T of both intervals exhibits the same pattern (Fig. DR2 [see footnote 1]). Abiotic here refers to ooids, peloids, and intraclasts. A detailed explanation is provided in Table DR1.

studied sections. Fe_{HR}/Fe_T and autotroph content exhibit a significant polynomial relationship (Fig. 2). Autotrophic content increases with Fe_{HR}/Fe_T in samples with Fe_{HR}/Fe_T <0.5, whereas autotrophic content remains high and relatively invariant in samples with Fe_{HR}/Fe_T >0.5 (Fig. 2).

The size distribution of the dust varies from a minority (<4%) of short-range-transported coarse particles (15–120 µm) to a majority of long-range-transported fine particles (<15 µm). The coarsest grains (>63 µm) are commonly well rounded, inferred to represent eolian sand that accumulated near shore, and finer grains represent particles potentially sourced from regions >10^3 km distant. The samples with a larger proportion of fine dust (<31 µm) have significantly higher Fe_{HR}/Fe_T values, and positively covary with autotroph content (Fig. 3). These samples are also enriched in Fe_{HR}, whereas facies with low or minimal autotroph content exhibit lower Fe_{HR}. Moreover, samples dominated by fine dust (<31 µm) are enriched in Fe_{HR} without a corresponding increase in Fe_T.

DISCUSSION

Autotrophic predominance increases with Fe_{HR} which corresponds with fine (<31 µm) dust in the study region. Considering the sample location, these results highlight dust as the primary input of Fe_{HR} into the carbonate platforms of the Central Persian terrane during the Late Pennsylvanian–early Permian. Furthermore, the high values of 2-MHI indicate a large contribution of cyanobacteria to the organic matter, which can drive fixation of local nitrogen—an important macronutrient. Quantification of the autotrophic content via both the biomarker index (2-MHI) and the point-count results reveals a robust positive relationship between dust-borne Fe_{HR}, autotrophic activity, and carbonate precipitation.

The Fe_{HR}/Fe_T values range from 0.1 to 1, with an average of ~0.7, similar to those reported from eolian-transported upper Gzhelian mudstone of western equatorial Pangaea (Sur et al., 2015). The Fe_{HR}/Fe_T values reported here significantly exceed values reported from Saharan soil dust (0.33 ± 0.01 standard error [SE]: Poulton and Raiswell, 2002; 0.37 ± 0.03 SE: Raiswell et al., 2016). Our values are more similar to those from modern euxinic settings, such as the Black Sea and the Cariaco Basin (offshore Venezuela) (Raiswell and Canfield, 1996), even though low Fe_{py}/Fe_T indicates mildly reducing conditions in the Central Persian terrane during the late Paleozoic. The Fe_T/Al values range from 0.22 to 6.91 (average 3.8), and importantly, the Fe reactivity decreases with increasing Fe_T/Al (R^2 = 0.18; *F*-test statistic of a linear regression [*F*] = 10.4, degrees of freedom [df] = (1,48); *P* = 0.002).

Figure 1B illustrates variation in Fe_{HR}/Fe_T, fine-dust and autotroph content across the

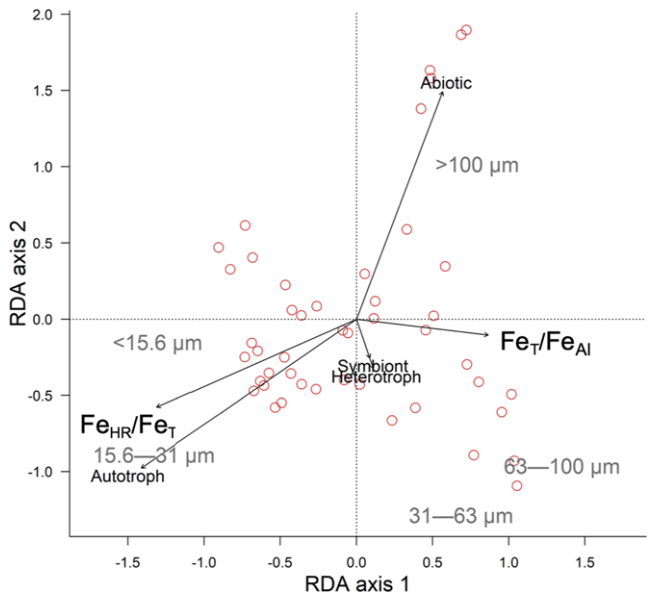

Figure 3. Redundancy analysis (RDA) visualizing the relationships among the proportion of highly reactive Fe (Fe_{HR}) over total Fe (Fe_T), dust grain size (in µm), and proportions of biotic and abiotic components in peri-Gondwanan terranes of Iran. Each point (red circle) indicates an individual sample. Closer proximity to a given predictor or driver variable indicates higher values of that variable for the sample.

Increasing Fe_{HR} with decreasing Fe_T/Al likely indicates significant influence of non-aluminosilicate (clastic) sources predominated by iron-oxide-rich dust.

Fine dust lingers in suspension, and is subject to more cloud processing and can be transported greater distances compared to coarser particles. Enhanced bioavailability of Fe in finer-grained dust likely reflects both longer residence time in the water column and greater surface area, which increases the potential for biological and/or chemical alterations. The sample location is near a predicted upwelling zone (Golonka et al., 1994) and where a warm western boundary current and a polar front may have met (Sardar Abadi et al., 2019), so mesoscale eddies could have brought non-Fe nutrients into the area (Garçon et al., 2001). However, neither upwelling nor hydrothermal sources for Fe are consistent with either the facies data or the predominance of iron oxide. Additionally, because the local continental margin was isolated from fluvial sources of Fe, greater non-Fe nutrient input from coastal waters would have enhanced Fe limitation (Hogle et al., 2018).

The hypothesis that Fe-rich dust stimulated productivity, enhancing carbon burial and decreasing atmospheric CO_2, explains a major quandary in understanding pCO_2 during the waning stages of the LPIA: namely, the disconnect between evidence for carbon sequestration on land and trends in atmospheric pCO_2. Atmospheric pCO_2 reaches a nadir near the Pennsylvanian-Permian boundary, even though the hypothesized drivers of decreasing pCO_2 for this interval—namely, peak coal burial and continental weathering—occurred in the Early to Middle Pennsylvanian (Fig. 4; Montañez et al., 2016; Nelsen et al., 2016; Goddéris et al., 2017; Chen et al., 2018). Chen et al. (2018) inferred a shift in the locus of carbon burial from the terrestrial to the marine biosphere during this interval, consistent with the results of Sur et al. (2015) who posited substantial fertilization of the marine biosphere by iron-rich dust. Indeed, the onset of aridification during the Late Pennsylvanian is consistent with an increase in atmospheric dustiness during the LPIA (Heavens et al., 2015; Soreghan et al., 2015), which likely stimulated *marine* productivity, shifting carbon burial from the continental to the marine realm (Sur et al., 2015; Chen et al., 2018).

Sur et al. (2015) documented eolian delivery of Fe_{HR} to equatorial western Pangaea during the Late Pennsylvanian (Gzhelian) and speculated on the potential for large repercussions to carbon cycling if this phenomenon were more widespread. The high values of Fe_{HR} in southern mid-latitudes extend Sur et al.'s (2015) results both temporally and spatially. Furthermore, these data represent the first documentation of a positive covariance in marine autotrophs and bioavailable Fe delivered by dust in Earth's deep-time record. Our findings document the ecosystem dependence on dust inputs and demonstrate the viability of the late Paleozoic dust fertilization hypothesis for helping to explain prolonged drawdown of pCO_2 at peak LPIA. Importantly, a shift in the locus (e.g., terrestrial to marine) of organic carbon burial likely has an insignificant effect on the global carbon isotope record, however a small trend toward more positive values (Chen et al., 2018) may suggest an increase in global organic carbon burial, which would correspond with a decrease in pCO_2. A similar effect has been observed for a Mesozoic event (Jarvis et al., 2011). Additionally, a positive carbon isotope excursion could be dampened by enhanced volcanism and/or increased weathering, both of which have been implicated during this interval (Goddéris et al., 2017; Soreghan et al., 2019); thus, our interpretation is consistent with the known carbon isotope record (Chen et al., 2018).

The remarkably high values of Fe_{HR} documented in both Sur et al.'s (2015) and our data sets imply an enhancement of reactive (and thus bioavailable) Fe for atmospheric aerosols of the LPIA. The mechanism behind this enhancement has been enigmatic. More recently, however, Soreghan et al. (2019) documented high amounts of explosive volcanism during the LPIA and linked this to increased atmospheric acidity and consequent enhancement of the reactivity of Fe in mineral aerosols. This mechanism would strengthen carbon burial by both stimulating primary producers and—as an auxiliary effect—enhancing microbial carbonate precipitation.

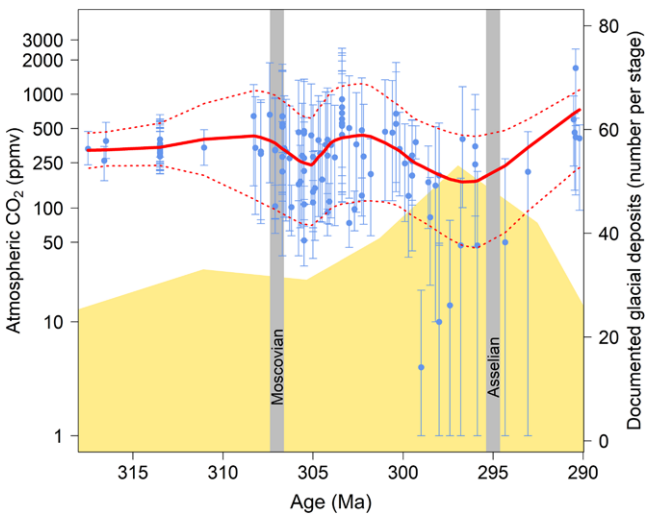

Figure 4. Reconstructed atmospheric pCO_2 between 318 and 290 Ma (Montañez et al., 2007, 2016). Solid red line represents loess fit with 50% smoothing, and dashed red lines represent loess fit of upper and lower confidence-interval values. Documented glacial deposits are illustrated with yellow polygon (Soreghan et al., 2019). Gray bars lines refer to case studies.

CONCLUSIONS

Atmospheric dust delivered Fe_{HR} to epeiric seas of southern mid-latitude Pangaea during the LPIA, stimulating marine primary (autotrophic) productivity. Fe_{HR} borne by (especially) the finest dust enhanced microbial and cyanobacterial growth, promoting both carbonate precipitation and marine C_{org} burial. Consequently, dust likely stimulated both organic and inorganic carbon cycling, helping to maintain low pCO_2 even as terrestrial repositories for organic carbon (peat and/or coal) and silicate weathering diminished from the Carboniferous into the Permian.

ACKNOWLEDGMENTS

This research was supported by the U.S. National Science Foundation (grants EAR-1338331 and EAR–1337463 to Soreghan). Owens acknowledges support from the NASA Exobiology program (NNX16AJ60G and 80NSSC18K1532). We thank A. Ridgwell, R. Raiswell, C. Fielding, and two anonymous reviewers for constructively critical reviews, and J. Schmitt for editorial handling.

REFERENCES CITED

Boyd, P.W., et al., 2004, The decline and fate of an iron-induced subarctic phytoplankton bloom: Nature, v. 428, p. 549–553, https://doi.org/10.1038/nature02437.

Bressac, M., Guieu, C., Doxaran, D., Bourrin, F., Desboeufs, K., Leblond, N., and Ridame, C., 2014, Quantification of the lithogenic carbon pump following a simulated dust-deposition event in large mesocosms: Biogeosciences, v. 11, p. 1007–1020, https://doi.org/10.5194/bg-11-1007-2014.

Chen, J., Montañez, I.P., Qi, Y., Shen, S., and Wang, X., 2018, Strontium and carbon isotopic evidence for decoupling of pCO_2 from continental weathering at the apex of the late Paleozoic glaciation: Geology, v. 46, p. 395–398, https://doi.org/10.1130/G40093.1.

Chien, C.-T., Mackey, K.R., Dutkiewicz, S., Mahowald, N.M., Prospero, J.M., and Paytan, A., 2016, Effects of African dust deposition on phytoplankton in the western tropical Atlantic Ocean off Barbados: Global Biogeochemical Cycles, v. 30, p. 716–734, https://doi.org/10.1002/2015GB005334.

Garçon, V.C., Oschlies, A., Doney, S.C., McGillicuddy, D.J., and Waniek, J., 2001, The role of mesoscale variability on plankton dynamics in the North Atlantic: Deep-Sea Research: Part II, Topical Studies in Oceanography, v. 48, p. 199–226, https://doi.org/10.1016/S0967-0645(00)00183-1.

Goddéris, Y., Donnadieu, Y., Carretier, S., Aretz, M., Dera, G., Macouin, M., and Regard, V., 2017, Onset and ending of the late Palaeozoic ice age triggered by tectonically paced rock weathering: Nature Geoscience, v. 10, p. 382–386, https://doi.org/10.1038/ngeo2931.

Golonka, J., Ross, M.I., and Scotese, C.R., 1994, Phanerozoic paleogeographic and paleoclimatic modeling maps, *in* Embry, A.F., et al., eds., Pangea: Global Environments and Resources: Canadian Society of Petroleum Geologists Memoir 17, p. 1–47.

Groß, J., 2003, Variance inflation factors: R News: The Newsletter of the R Project, v. 3, no. 1, p. 13–15.

Guieu, C., Ridame, C., Pulido-Villena, E., Bressac, M., Desboeufs, K., and Dulac, F., 2014, Impact of dust deposition on carbon budget: A tentative assessment from a mesocosm approach: Biogeosciences, v. 11, p. 5621–5635.

Guo, C., Yu, J., Ho, T.-Y., Wang, L., Song, S., Kong, L., and Liu, H., 2012, Dynamics of phytoplankton community structure in the South China Sea in response to the East Asian aerosol input: Biogeosciences, v. 9, p. 1519–1536, https://doi.org/10.5194/bg-9-1519-2012.

Hauck, J., Köhler, P., Wolf-Gladrow, D., and Völker, C., 2016, Iron fertilisation and century-scale effects of open ocean dissolution of olivine in a simulated CO_2 removal experiment: Environmental Research Letters, v. 11, 024007, https://doi.org/10.1088/1748-9326/11/2/024007.

Heavens, N.G., Mahowald, N.M., Soreghan, G.S., Soreghan, M.J., and Shields, C.A., 2015, A model-based evaluation of tropical climate in Pangaea during the late Palaeozoic icehouse: Palaeogeography, Palaeoclimatology, Palaeoecology, v. 425, p. 109–127, https://doi.org/10.1016/j.palaeo.2015.02.024.

Hogle, S.L., et al., 2018, Pervasive iron limitation at subsurface chlorophyll maxima of the California Current: Proceedings of the National Academy of Sciences of the United States of America, v. 115, p. 13,300–13,305, https://doi.org/10.1073/pnas.1813192115.

IPCC (Intergovernmental Panel on Climate Change), 2018, Global warming of 1.5°C: An IPCC Special Report on the impacts of global warming of 1.5°C above pre-industrial levels and related global greenhouse gas emission pathways, in the context of strengthening the global response to the threat of climate change, sustainable development, and efforts to eradicate poverty: Geneva, World Meteorological Organization, 616 p.

Jarvis, I., Lignum, J.S., Gröcke, D.R., Jenkyns, H.C., and Pearce, M.A., 2011, Black shale deposition, atmospheric CO_2 drawdown, and cooling during the Cenomanian-Turonian Oceanic Anoxic Event: Paleoceanography, v. 26, PA3201, https://doi.org/10.1029/2010PA002081.

Krishnamurthy, A., Moore, J.K., Mahowald, N., Luo, C., and Zender, C.S., 2010, Impacts of atmospheric nutrient inputs on marine biogeochemistry: Journal of Geophysical Research, v. 115, G01006, https://doi.org/10.1029/2009JG001115.

Legendre, P., and Legendre, L., 1998, Numerical Ecology (second English edition): Amsterdam, Elsevier, 852 p.

Martin, J.H., 1990, Glacial-interglacial CO_2 change: The iron hypothesis: Paleoceanography, v. 5, p. 1–13, https://doi.org/10.1029/PA005i001p00001.

Montañez, I.P., Tabor, N.J., Niemeier, D., DiMichele, W.A., Frank, T.D., Fielding, C.R., Isbell, J.L., Birgenheier, L.P., and Rygel, M.C., 2007, CO_2-forced climate and vegetation instability during Late Paleozoic deglaciation: Science, v. 315, p. 87–91, https://doi.org/10.1126/science.1134207.

Montañez, I.P., McElwain, L.C., Poulsen, C.J., White, J.D., DiMichele, W.A., Wilson, J.P., Griggs, G., and Hren, M.T., 2016, Climate, pCO_2 and terrestrial carbon cycle linkages during late Palaeozoic glacial–interglacial cycles: Nature Geoscience, v. 9, p. 824–828, https://doi.org/10.1038/ngeo2822.

Nelsen, M.P., DiMichele, W.A., Peters, S.E., and Boyce, C.K., 2016, Delayed fungal evolution did not cause the Paleozoic peak in coal production: Proceedings of the National Academy of Sciences of the United States of America, v. 113, p. 2442–2447, https://doi.org/10.1073/pnas.1517943113.

Oksanen, J., et al., 2018, vegan: Community ecology package: R package, version 2.5-1: https://CRAN.R-project.org/package=vegan (accessed July 2019).

Poulton, S.W., and Canfield, D.E., 2005, Development of a sequential extraction procedure for iron: Implications for iron partitioning in continentally derived particulates: Chemical Geology, v. 214, p. 209–221, https://doi.org/10.1016/j.chemgeo.2004.09.003.

Poulton, S.W., and Raiswell, R., 2002, The low-temperature geochemical cycle of iron: From continental fluxes to marine sediment deposition: American Journal of Science, v. 302, p. 774–805, https://doi.org/10.2475/ajs.302.9.774.

Raiswell, R., and Canfield, D.E., 1996, Rates of reaction between silicate iron and dissolved sulfide in Peru Margin sediments: Geochimica et Cosmochimica Acta, v. 60, p. 2777–2787, https://doi.org/10.1016/0016-7037(96)00141-X.

Raiswell, R., et al., 2016, Potentially bioavailable iron delivery by iceberg-hosted sediments and atmospheric dust to the polar oceans: Biogeosciences, v. 13, p. 3887–3900, https://doi.org/10.5194/bg-13-3887-2016.

Raiswell, R., Hardisty, D.S., Lyons, T.W., Canfield, D.E., Owens, J.D., Planavsky, N.J., Poulton, S.W., and Reinhard, C.T., 2018, The iron paleoredox proxies: A guide to the pitfalls, problems and proper practice: American Journal of Science, v. 318, p. 491–526, https://doi.org/10.2475/05.2018.03.

R Core Team, 2019, R: A language and environment for statistical computing: Vienna, Austria, Foundation for Statistical Computing, https://www.R-project.org/.

Sardar Abadi, M., Soreghan, G.S., Heavens, N.G., Voeten, D.F., and Ivanova, R.M., 2019, Warm-water carbonates in proximity to Gondwanan ice-sheets: A record from the Upper Paleozoic of Iran: Palaeogeography, Palaeoclimatology, Palaeoecology, v. 531, 108914, https://doi.org/10.1016/j.palaeo.2018.09.008.

Schlager, W., 2003, Benthic carbonate factories of the Phanerozoic: International Journal of Earth Sciences, v. 92, p. 445–464, https://doi.org/10.1007/s00531-003-0327-x.

Soreghan, G.S., Soreghan, M.J., and Hamilton, M.A., 2008, Origin and paleoclimatic significance of tropical silt in the late Paleozoic icehouse: Palaeogeography, Palaeoclimatology, Palaeoecology, v. 268, p. 234–259, https://doi.org/10.1016/j.palaeo.2008.03.050.

Soreghan, G.S., Heavens, N.G., Hinnov, L.A., Aciego, S.M., and Simpson, C., 2015, Reconstructing the dust cycle in deep time: The case of the late Paleozoic icehouse, *in* Polly, P.D., et al., eds., Earth-Life Transitions: Paleobiology in the Context of Earth System Evolution: The Paleontological Society Papers, v. 21, p. 83–120, https://doi.org/10.1017/S1089332600002977.

Soreghan, G.S., Soreghan, M.J., and Heavens, N.G., 2019, Explosive volcanism as a key driver of the late Paleozoic ice age: Geology, v. 47, p. 600–604, https://doi.org/10.1130/G46349.1.

Summons, R.E., Jahnke, L.L., Hope, J.M., and Logan, G.A., 1999, 2-Methylhopanoids as biomarkers for cyanobacterial oxygenic photosynthesis: Nature, v. 400, p. 554–557, https://doi.org/10.1038/23005.

Sur, S., Soreghan, M.J., Soreghan, G.S., and Stagner, A.F., 2010, Extracting the silicate mineral fraction from ancient carbonate: Assessing the geologic record of dust: Journal of Sedimentary Research, v. 80, p. 763–769, https://doi.org/10.2110/jsr.2010.068.

Sur, S., Owens, J.D., Soreghan, G.S., Lyons, T.W., Raiswell, R., Heavens, N.G., and Mahowald, N.M., 2015, Extreme eolian delivery of reactive iron to late Paleozoic icehouse seas: Geology, v. 43, p. 1099–1102, https://doi.org/10.1130/G37226.1.

Swart, P.K., Oehlert, A.M., Mackenzie, G.J., Eberli, G.P., and Reijmer, J.J.G., 2014, The fertilization of the Bahamas by Saharan dust: A trigger for carbonate precipitation?: Geology, v. 42, p. 671–674, https://doi.org/10.1130/G35744.1.

Zhu, T., and Dittrich, M., 2016, Carbonate precipitation through microbial activities in natural environment, and their potential in biotechnology: A review: Frontiers in Bioengineering and Biotechnology, v. 4, 4, https://doi.org/10.3389/fbioe.2016.00004.

Printed in USA